GEOPHYSICAL RESEARCH LETTERS, VOL. 36, L11707, doi:10.1029/2009GL037832, 2009

Arctic stratospheric winter warming forced by observed SSTs

Yongyun Hu[1] and Lingfen Pan[1]

Received 19 February 2009; revised 10 April 2009; accepted 28 April 2009; published 10 June 2009.

[1] Observations showed warming trends in the Arctic stratosphere in early winter months in the past few decades, in contrast to cooling trends in late winter months mainly due to ozone depletion. To examine whether observed warming trends is caused by sea surface temperature (SST) increases, we analyze results from AMIP simulations which are forced by observed time-varying SSTs. It is found that all AMIP simulations demonstrate warming trends in the Arctic lower stratosphere. It also shows a weakened Arctic polar vortex, in responding to the polar warming. Empirical Orthogonal function (EOF) analysis shows a downward trend toward the negative polarity of an annular-like mode. Further analyses indicate that the Arctic stratospheric warming is associated with increasing wave activity and enhanced wave-flux convergence in the extratropical stratosphere, suggesting that the polar warming is caused by enhanced wave-driven adiabatic heating due to SST increases. **Citation:** Hu, Y., and L. Pan (2009), Arctic stratospheric winter warming forced by observed SSTs, *Geophys. Res. Lett.*, *36*, L11707, doi:10.1029/2009GL037832.

1. Introduction

[2] Observations showed warming trends in the stratospheric Arctic in early winter months (November and December) since the late 1970s [*Hu et al.*, 2005], in contrast to the cooling trends which are mainly caused by ozone depletion in late-winter months or spring [*Randel and Wu*, 1999]. Corresponding to the polar warming, the Northern-Hemisphere annular mode (NAM) displays negative trends, the polar night jet is decelerated, and wave activity is increased in the Northern-Hemisphere (NH) middle and high latitudes [*Hu and Tung*, 2003; *Karpetchko and Nikulin*, 2004; *Hu et al.*, 2005]. Warming trends are also found in the stratospheric Antarctic in austral winter and early spring [*Johanson and Fu*, 2007; *Hu and Fu*, 2009]. The stratospheric polar warming has important implication for polar ozone recovery because polar warming would reduce the formation of polar stratospheric clouds, which slows down the rates of heterogeneous chemical reactions and thus benefits the recovery of polar ozone, especially for the Antarctic ozone hole [*World Meteorological Organization*, 2007; *Hu and Fu*, 2009].

[3] The polar warming in the past few decades cannot be explained by radiative forcing on the stratosphere because the radiative effects of both ozone depletion and increasing greenhouse gases cause stratospheric cooling. Based on results from National Center for Environmental Prediction/National Center for Atmospheric Research (NCEP/NCAR) reanalysis [*Kalnay et al.*, 1996] and *Hu et al.* [2005] showed that the early-winter Arctic warming is associated with increasing wave activity in the stratosphere. Therefore, they suggested that the Arctic warming is due to enhanced wave-driven adiabatic heating. It is because increasing wave activity would lead to an intensified Brewer-Dobson circulation which has the downward branch in the stratospheric polar region. They further suggested that the increase in wave activity is likely forced due to sea surface temperature (SST) warming. Since SST warming is caused by the greenhouse effect due to increasing greenhouse gases [*Intergovernmental Panel on Climate Change*, 2007], the observed stratospheric polar warming is likely an integral part of global greenhouse warming. Using general circulation model (GCM) simulations, *Butchart and Scaife* [2001], *Eichelberger and Hartmann* [2005], and *Butchart et al.* [2006] showed that the Brewer-Dobson circulation is intensified, suggesting warming in the polar stratosphere. In studying Antarctic stratospheric warming in austral winter and early spring, *Hu and Fu* [2009] found that the observed Antarctic warming trend has close correlations with SSTs, especially tropical SSTs.

[4] To examine whether the observed stratospheric Arctic warming is forced by SST forcing and whether SST forcing can generate increasing wave activity in the stratosphere in winter, we analyze results from GCM simulations with SST forcing. Simulation data used in this study is described in section 2. Results are presented in section 3. Conclusions and discussion are summarized in section 4.

2. Data and Methods

[5] The data used in this study is GCM simulation results from the AMIP (atmospheric model intercomparison project) [*Gates et al.*, 1999]. AMIP was to simulate atmospheric responses to the observed sequence of monthly averaged global SST and sea-ice distributions during the 1980s–1990s, along with standardized values of the solar constant and atmospheric CO_2 concentration. Online available data are only from 10 GCMs. Among them, 5 GCMs have ensemble members of simulations (GISS, IAP, IPSL, MIROC, and MPI), and the other 5 have only single simulations (CNRM, GFDL, MRI, NCAR and UKMO). We choose MPI and NCAR outputs from the groups of ensemble mean simulations and single simulations as representatives of the full model ensemble, respectively. The simulation periods of these GCMs are slightly different. To avoid the differences, we convert all trends to a 20-year period (roughly 1980–1999). Therefore, the unit of temperature trends is °C per 20 years, and it is the same for other quantities. A weakness of using the AMIP simulations for studying stratospheric climate changes is that these models all have no full stratospheres and the top level of outputs

[1]Department of Atmospheric Sciences, School of Physics, Peking University, Beijing, China.

0094-8276/09/2009GL037832$05.00

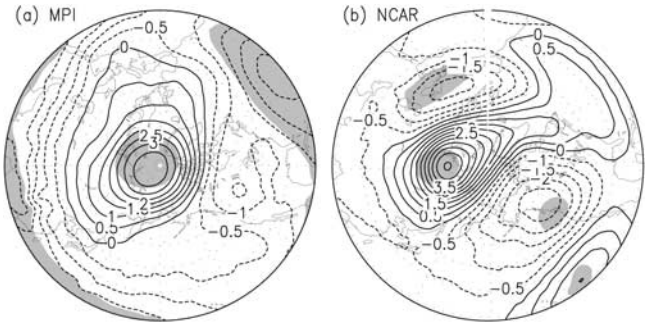

Figure 1. 20-year trends in temperatures at 50 hPa: (a) MPI and (b) NCAR. Solid contours, positive trends; dotted contours, negative trends. Contour interval is 0.5°C per 20 yr. Shading areas indicate the trends above the 90% confidence level (e.g., student's t-test value is greater than 1.7).

is 10 hPa. Nevertheless, the simulation results are reliable for studying the lower stratosphere that we are interested in because the GCMs all can well simulate the climatology of the lower stratosphere.

3. Results

[6] Figures 1a and 1b show the trends in temperatures at 50 hPa averaged over December–January–February (DJF), derived from MPI and NCAR simulations, respectively. For MPI ensemble mean simulations, NH high-latitudes are dominated by warming trends, with significant maximum warming of about 3.5°C over the 20 years right over the polar cap. In contrast, lower latitudes show relatively weak cooling. The NCAR single simulation also displays warming trends in the Arctic and cooling trends at middle latitudes, with a smaller warming area but greater warming magnitudes. The simulated DJF maximum warming trends in both ensemble and single simulations are comparable to that in reanalysis, which show a maximum warming of about 3.5°C, averaged over November and December, over the 21 years (1979–1999).

[7] Maximum polar warming trends at 50 hPa for all the 10 GCMs are summarized in Table 1. Let us first look at the seasonal maximum warming. For ensemble mean simulations, MPI yields the largest maximum warming of about 3.5°C over the 20 years, GISS has the smallest value of 0.5°C, and the other 3 models reproduce maximum warming of about 2°C. Averagely, ensemble mean simulations generated 2°C maximum warming over 20 years, weaker than that in reanalysis. For single simulations, NCAR, UKMO and MRI generated maximum warming of about 4–5°C, while GFDL and CNRM have relatively weak maximum warming of about 1–2°C. The averaged value of the 5 GCMs is about 3.5°C, same as that in reanalysis. For monthly mean, ensemble mean simulations produced maximum polar warming varying from 2.5 to 5.5°C, and single simulations generated maximum warming ranging from 5.5 to 7.0°C. The weaker warming in ensemble mean simulations is because ensemble averaging reduces warming amplitudes in individual simulations, which are dominated by chaotic, nonlinear atmospheric interactions [*Hoerling et al.*, 2001]. From the third column, one can find that the maximum polar warming can occur in any winter months (November–February). This is unlike observations in which warming mainly occurs in November and December, and cooling occurs in boreal spring because of ozone depletion [*Randel and Wu*, 1999; *Hu and Tung*, 2003; *Hu et al.*, 2005]. This suggests that in the absence of ozone depletion SST warming tends to generate Arctic stratospheric warming in all winter months.

[8] The polar warming suggests a weakening of the polar vortex and thus a downward trend toward the negative polarity of NAM. To show this, we carried out empirical orthogonal function (EOF) analysis for 50 hPa geopotential heights in winter months (October–March). Figures 2a and 2b show spatial patterns of the positive phase for the first EOF modes derived from MPI and NCAR simulations, respectively. They all show seesaw patterns, with low in the polar region and high in middle latitudes. The spatial patterns resemble that of the observed NAM. The first EOF modes can explain 31.2% and 40.8% of variances of 50 hPa geopotential heights for MPI and NCAR simulations, respectively. Both percentages are lower than that in NCEP/NCAR reanalysis, which is about 54% [*Thompson and Wallace*, 2000]. Figures 2c and 2d show the time series of the principal components. Both show negative trends over the 20 years. MPI yields a statistically significant negative trend. The student's t–test value equals to 3.74. The negative trend in NCAR simulation has lower statistical significance due to relatively large interannual fluctuations in the single simulation.

[9] To demonstrate atmospheric responses to SST forcing at other levels, in Figures 3a and 3b we show vertical cross-sections of DJF trends in zonal-mean temperatures in NH. For MPI, warming trends are dominated in the polar lower-stratosphere, high-latitude troposphere (50°N–80°N) and subtropical troposphere (20°N–30°N), with maximum warming greater than 3°C located in the stratospheric Arctic (around 50 hPa). For NCAR, the Arctic lower-stratosphere also demonstrates warming trends. However, the

Table 1. Summary of Maximum Polar Warming Trends at 50 hPa and Maximum Zonal-Mean Zonal Wind Trends for All AMIP GCMs[a]

	DJF ΔT (°C)	Monthly ΔT (°C)	DJF ΔU (m/s)
		Ensemble	
MPI	3.5	5.5(Dec)	−6.0
IAP	2.0	3.0(Nov)	−3.5
IPSL	2.0	2.5 (Jan)	−1.0
MIROC	1.5	2.5 (Jan)	−1.0
GISS	0.5	2.5(Feb)	0.5
		Single	
NCAR	5.0	6.5(Dec)	−5.0
MRI	5.0	7.0(Feb)	−5.0
UKMO	4.0	6.5(Feb)	−2.0
CNRM	2.0	5.5(Feb)	−5.0
GFDL	1.0	5.5(Feb)	0.0

[a]The top of the table shows ensemble mean simulations, and the bottom shows single simulations. The second column shows DJF-mean maximum warming in the polar region. The third column shows monthly maximum warming, and the months in which maximum warming occurs are provided in parentheses. The fourth column shows DJF-mean maximum zonal-mean zonal wind trends in the middle and high-latitude stratosphere.

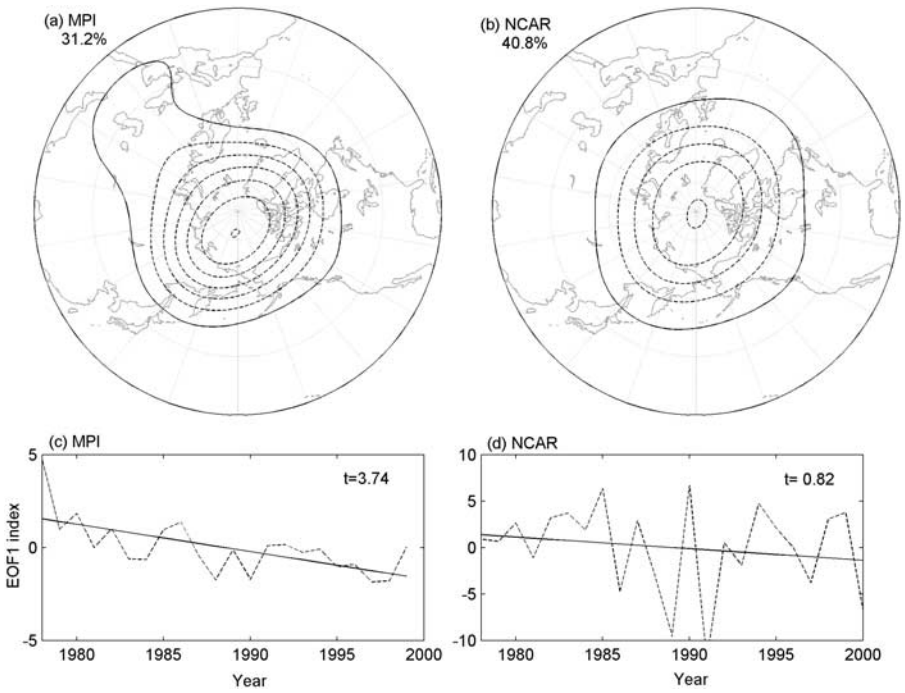

Figure 2. (top) Spatial patterns of the first EOF modes of 50 hPa geopotential heights and (bottom) time series of the principal components. Student's t-test values for trends are marked in the right upper corners.

warming trends are less significant due to large interannual fluctuations.

[10] Polar stratospheric warming must lead to reduced temperature contrast between the polar region and middle latitudes. According to the thermal-wind relation, the reduction of temperature contrast would cause decelerated zonal winds in the sub-polar region, i.e., polar night jet. To demonstrate this, we calculate trends in zonal-mean zonal winds, which are shown in Figures 3c and 3d, respectively. For MPI, significant negative trends are found in middle and

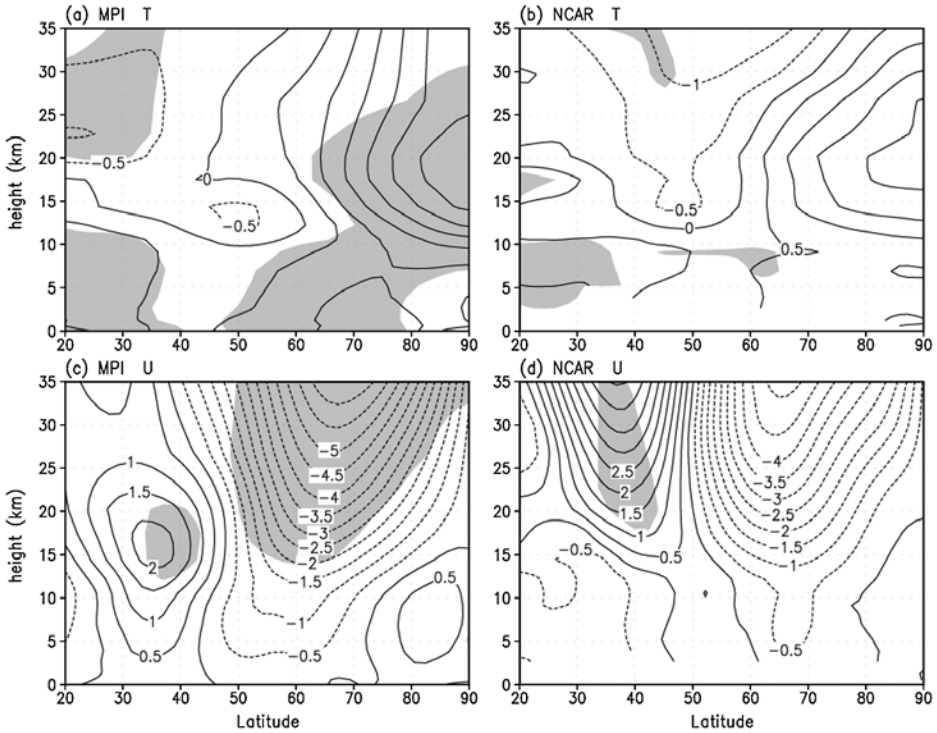

Figure 3. Trends in (a, b) zonal-mean temperatures and (c, d) zonal-mean zonal winds. Solid contours, positive trends; dotted-contours, negative trends. Shaded areas indicate the trends above the 90% confidence level.

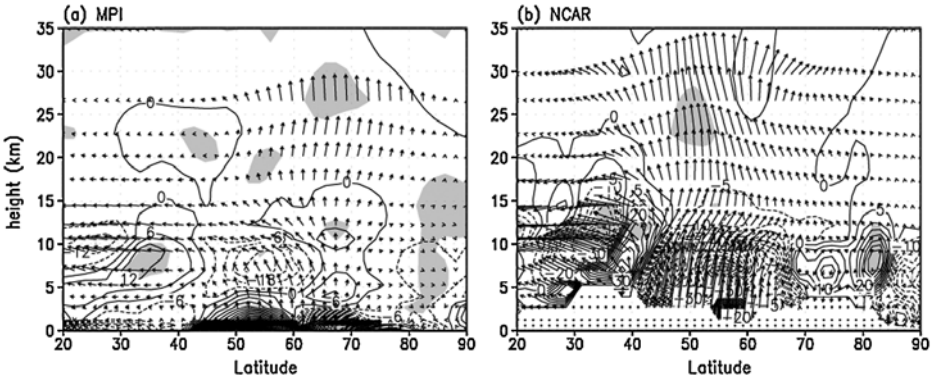

Figure 4. Trends in EP flux vectors and EP flux divergence: (a) MPI, and (b) NCAR. Arrows indicate trends in EP flux vectors. The scaling length of the arrows, 1 inch or 2.54 cm, represents 1.5×10^8 $m^3 s^{-2}$ per 20 yr. EP fluxes are divided by background air density, and the vertical component of EP flux vectors is multiplied by 100. Contours are trends in EP flux divergence. Solid lines, positive trends; dotted lines, negative trends. Contour interval is 5 m^2 s^{-2} per 25 yr. Shading areas indicate the trends in EP flux divergence above the 90% confidence level.

high latitudes in the stratosphere, which is indicative of deceleration of the polar night jet. The maximum deceleration of zonal winds is about 6 ms^{-1} over the 20 years, similar to that in reanalysis [see *Hu et al.*, 2005, Figure 4a]. The trends in NCAR are similar to that in MPI, except for that the negative trends are less significant. Trends in DJF zonal-mean zonal winds in other models are given in Table 1 (third column). They generally show zonal-wind deceleration, except for GISS and GFDL which show very weak trends in zonal winds.

[11] An important question is whether the simulated Arctic warming is caused by wave-driven adiabatic warming under the condition of SST forcing. Therefore, it is important to examine changes in wave fluxes, i.e., Eliassen-Palm (EP) fluxes in AMIP simulations. EP fluxes are usually calculated using daily wind and temperature data, which includes contribution from both transient and quasi-stationary waves. Because AMIP simulations have only monthly data available, the EP fluxes here are equivalent to quasi-stationary wave fluxes.

[12] Figure 4 shows the trends in EP flux vectors (arrows) and EP flux divergence (contours). For both MPI and NCAR, the upward arrows between about 40°N and 70°N indicate enhanced upward wave propagation, and the equatorward arrows in the extratropical upper troposphere indicate enhanced equatorward wave propagation. These suggest that there is increasing wave activity in both the extratropical troposphere and stratosphere, and that the source of increasing wave activity is in the lower troposphere between about 40°N and 70°N. What corresponds to the increasing wave activity is enhanced EP flux convergence in the middle and high-latitude stratosphere for MPI and in the extratropical troposphere and stratosphere for NCAR. The increases in both EP fluxes and EP flux divergence are qualitatively consistent with observations [see *Hu et al.*, 2005, Figure 6a]. According to the theory of wave-mean flow interaction, the enhancement of EP flux convergence in the extratropical stratosphere would cause decelerated zonal winds, intensified Brewer-Dobson circulation, and thus stronger adiabatic warming in the Arctic stratosphere. Comparison with Figure 3 shows consistency between the trends in EP fluxes and warming in the stratospheric Arctic as well as the deceleration of zonal winds in the middle and high-latitude stratosphere.

4. Conclusions and Discussion

[13] Using AMIP simulation results, we have shown that the observed stratospheric Arctic warming in early winter in the past few decades can be reasonably reproduced by observed global time-varying SST forcing. 5 GCMs with ensemble mean simulations yield averaged maximum warming of about 2.0°C in DJF over 1979–1999, weaker than observations, and the other 5 GCMs with single simulations display realistic magnitudes of maximum warming, about 3.5°C. The simulations also show that the polar night jet is decelerated, and that the simulated NAM demonstrates trends toward the negative polarity. It is found that the linkage between stratospheric Arctic warming and SST warming is through changes in atmospheric wave activity. Our analyses show that there are increases in EP fluxes in both the troposphere and stratosphere. It is the increase in wave fluxes and the enhancement of EP flux convergence that lead to wave-driven adiabatic warming in the stratospheric Arctic. These results confirm that SST warming is indeed a major factor in causing the observed warming in the stratospheric Arctic.

[14] The stratospheric Arctic warming in AMIP simulations are consistent with the simulation results of intensified Brewer-Dobson circulation of *Butchart and Scaife* [2001], *Eichelberger and Hartmann* [2005], and *Butchart et al.* [2006]. While all the simulation results agree that the Arctic warming or intensified Brewer-Dobson circulation are caused by increasing wave fluxes, they emphasize different forcing mechanisms in causing increasing wave fluxes. In the simple GCM simulations by *Eichelberger and Hartmann* [2005], the external forcing is increasing greenhouse gases. Increasing wave activity is a response to tropical tropospheric warming. The relatively strong warming in the tropical troposphere causes increasing mid-latitude baroclinicity, which consequently leads to an increase in synoptic and planetary wave activity. The results of *Butchart and Scaife* [2001] and *Butchart et al.* [2006] are from GCM simulations with full stratospheres. In these simulations, external forcing

includes both increasing greenhouse gases and observed or simulated time-varying SSTs. Therefore, increasing wave activity is caused by both factors. By contrast, the AMIP simulations has only SST forcing.

[15] A noticed difference of trends in EP flux vectors between AMIP simulations and reanalysis is that the horizontal component of trends in EP flux vectors in AMIP simulations is generally equatorward in the extratropical upper troposphere, whereas it is poleward in reanalysis [see *Hu et al.*, 2005, Figure 6a]. The difference suggests different sources for increasing wave activity. AMIP simulations indicate a source of increasing wave activity in the extratropical troposphere. In contrast, results from reanalysis suggest a source in the tropics. *Hoerling et al.* [2001], *Li et al.* [2006], and *Li* [2009] argued that decadal changes in the extratropical atmosphere are mainly originated from tropical SST forcing, while SSTs over other regions have minor forcing on the atmosphere. They showed that tropical SST warming, throughout deep convections and strong latent heat release, would excite stronger waves in the extratropics and thus modulate extratropical atmospheric circulations and climate. Whether the source of increasing wave activity is in the tropics or extratropics needs further studies, in which contributions from transient waves have to be included.

[16] **Acknowledgments.** This work is supported by the NSF of China (40875042 and 40533016), and the Ministry of Education of China (20070001002).

References

Butchart, N., and A. A. Scaife (2001), Removal of chlorofluorocarbons by increased mass exchange between the stratosphere and troposphere in a changing climate, *Nature*, *410*, 799–802.

Butchart, N., et al. (2006), Simulations of anthropogenic change in the strength of the Brewer-Dobson circulation, *Clim. Dyn.*, *27*, 727–741.

Eichelberger, S. J., and D. L. Hartmann (2005), Changes in the strength of the Brewer-Dobson circulation in a simple AGCM, *Geophys. Res. Lett.*, *32*, L15807, doi:10.1029/2005GL022924.

Gates, W. L., et al. (1999), An overview of the results of the atmospheric model intercomparison project (AMIP I), *Bull. Am. Meteorol. Soc.*, *80*, 29–55.

Hoerling, M. P., W. Hurrell, and T. Xu (2001), Tropical origins for recent North Atlantic climate change, *Science*, *292*, 90–92.

Hu, Y., and Q. Fu (2009), Antarctic stratospheric warming since 1979, *Atmos. Chem. Phys. Discuss.*, *9*, 1–24.

Hu, Y., and K. K. Tung (2003), Possible ozone induced long-term changes in planetary wave activity in late winter, *J. Clim*, *16*, 3027–3038.

Hu, Y., K. K. Tung, and J. Liu (2005), A closer comparison of decadal atmospheric trends between Northern-Hemisphere early and late winter, *J. Clim.*, *18*, 3204–3216.

Intergovernmental Panel on Climate Change (2007), *Climate Change 2007: The Physical Basis*, edited by S. Solomon et al., Cambridge Univ. Press, Cambridge, U. K.

Johanson, C. M., and Q. Fu (2007), Antarctic atmospheric temperature trend patterns from satellite observations, *Geophys. Res. Lett.*, *34*, L12703, doi:10.1029/2006GL029108.

Kalnay, E., et al. (1996), The NCEP/NCAR 40-year reanalysis project, *Bull. Am. Meteorol. Soc.*, *77*, 437–471.

Karpetchko, A., and G. Nikulin (2004), Influence of early winter upward wave activity flux on midwinter circulation in the stratosphere and troposphere, *J. Clim.*, *17*, 4443–4452.

Li, S. (2009), Influence of tropical Indian Ocean warming on the stratospheric southern polar vortex, *Sci. China, Ser. D*, *52*, 323–332.

Li, S., et al. (2006), The annular response to tropical Pacific SST forcing, *J. Clim.*, *19*, 1802–1819.

Randel, W. J., and F. Wu (1999), Cooling of the Arctic and Antarctic polar stratospheres due to ozone depletion, *J. Clim.*, *12*, 1467–1479.

Thompson, D. W. J., and J. M. Wallace (2000), Annular modes in the extratropical circulation, Part I: Month-to-month variability, *J. Clim.*, *13*, 1000–1016.

World Meteorological Organization (2007), *Scientific Assessment of Ozone Depletion—2006*, *Global Ozone Res. Monit. Proj. Rep. 50*, Geneva, Switzerland.

Y. Hu and L. Pan, Department of Atmospheric Sciences, School of Physics, Peking University, Beijing, 100871, China. (yyhu@pku.edu.cn)